

Meissner effect in honeycomb arrays of multiwalled carbon nanotubes

N. Murata,^{1,4} J. Haruyama,^{1,4,*} Y. Ueda,¹ M. Matsudaira,¹ H. Karino,¹ Y. Yagi,⁴ E. Einarsson,² S. Chiashi,² S. Maruyama,² T. Sugai,^{3,4} N. Kishi,³ and H. Shinohara^{3,4}

¹*Aoyama Gakuin University, 5-10-1 Fuchinobe, Sagamihara, Kanagawa 229-8558 Japan*

²*Tokyo University, 7-3-1 Hongo, Bunkyo-ku, Tokyo 113-0033 Japan*

³*Nagoya University, Furo-cho, Chigusa, Nagoya 464-8602 Japan*

⁴*JST-CREST, 4-1-8 Hon-machi, Kawaguchi, Saitama 332-0012 Japan*

(Received 2 October 2007; published 20 December 2007)

We report a gradual magnetization drop with an onset temperature (T_c) of 18–23 K found in the honeycomb arrays of multiwalled CNTs (MWNTs) showing a slight resistance decrease due to superconductivity. Magnetic field dependence of the drop and temperature dependence of critical fields indicate that it is attributed to Meissner effect for type-II superconductors. The T_c value is the highest among those in new carbon-related superconductors. The weak magnetic anisotropy, superconductive coherence length (11–19 nm), and disappearance of the Meissner effect after destructing array structure suggest that intertube coupling of MWNTs in the honeycomb array is a dominant factor for the mechanism. Drastic reduction of ferromagnetic catalyst for synthesis of the MWNTs makes the finding possible.

DOI: 10.1103/PhysRevB.76.245424

PACS number(s): 74.70.Wz, 74.78.Na

I. INTRODUCTION

New carbon-based superconductors, such as C_6Ca with a transition temperature (T_c) of 11.5 K,^{1,2} and highly boron-doped diamond with $T_c=4$ K,³ have been recently found and attracted considerable attention, because a small mass of carbon may lead to high- T_c superconductivity (SC) such as MgB_2 . SC in carbon nanotubes (CNTs) has also attracted increasing attention.^{4–7} Three groups have experimentally reported SC in different kinds of CNTs; (1) with a T_c as low as 0.4 K for resistance drops (T_{cR}) in ropes of single-walled CNTs (SWNTs),^{4,5} (2) with a T_{cR} as high as 12 K for an abrupt resistance drop in arrays of our multiwalled CNTs (MWNTs) entirely end-bonded by gold electrode,⁶ (3) with a T_c of 15 K for magnetization drops (T_{cH}) in SWNTs with diameters as small as 0.4 nm.⁷ However, no groups could report both the Meissner effect and the resistance drop down to 0 Ω in their respective CNT systems.⁸

One of main reasons for difficulty in observation of Meissner effect in CNTs is that most high-quality CNTs have been synthesized using ferromagnetic catalysts (e.g., Fe, Co, Ni) in previous studies. Such catalysts remain in the CNTs even after synthesis in some cases and destroy Meissner effect. In particular, measurements of resistance and magnetization have very different aspect in our array of MWNTs. SC for resistance drops could be observed if even only one MWNT without Fe/Co catalyst exists,⁶ because all supercurrent could flow through this MWNT. In contrast, for magnetization measurements, even very small amount of Fe/Co catalysts remaining in only one MWNT has obstructed observation of Meissner diamagnetism of the array. Hence, reduction of amount of Fe/Co is crucial.

Moreover, it is important to reveal how shielding currents for Meissner effect or superconducting vortices can occur and behave in one-dimensional (1D) space of CNTs, because discussion of correlation of superconductive coherence length with magnetic penetration length for conventional Meissner effect in 2D and 3D superconductors is not relevant

in CNTs with diameter as small as a few nm and tube structure. In contrast, it may be relevant in the case of coupled CNTs, which has 3D structures such as bundles or arrays. In fact, Ref. 5 reported possible Meissner effect in ropes of SWNTs.

II. SAMPLE FABRICATION AND STRUCTURE

In the present study, we have synthesized honeycomb arrays of high-quality MWNTs in nanopores of alumina template (Al_2O_3) by chemical vapor deposition (CVD) using Fe/Co catalyst and methanol (ethanol) gas, as shown in Fig. 1(a).⁶ Importantly, the amount of Fe/Co catalyst, which was electrochemically deposited into the bottom ends of nanopores, has been drastically reduced in order to detect the Meissner effect.⁹

For this purpose, we investigated the following three conditions for deposition. (1) Temperature (T_d) of solutions at 40–62 °C. (2) Deposition voltages (V_d) of 8–12 V. (3) Deposition time (t_d) for 3–20 s. The amount of catalyst drastically decreased by reduction of deposition energies and time; e.g., decrease in mass of Fe/Co was ~ 3 μg between the samples deposited by $T_d=62$ °C, $V_d=12$ V, $t_d=20$ s, and by $T_d=40$ °C, $V_d=8$ V, $t_d=3$ s. The decrease was also very evident in the colors of alumina templates surface right after deposition of Fe/Co; e.g., black (i.e., color of Fe/Co) in the samples deposited by the former conditions, while gold (i.e., color of alumina membrane) in that deposited by the latter conditions. Consequently, the best condition, which allows the smallest volume of Fe/Co, was determined as $T_d=40$ °C, $V_d=8$ V, and $t_d=3$ s.

However, it was found that amount of MWNTs synthesized in an alumina template was too small under this condition. Because the nanopores have high aspect ratio of length (~ 600 nm) and diameter (~ 10 nm), reaction for CVD with catalyst is not so active at the bottom ends of such nanopores. Thus, the reduced volume of Fe/Co catalyst makes synthesis of large amount of MWNTs difficult. In order to synthesize much larger volume of MWNTs under this

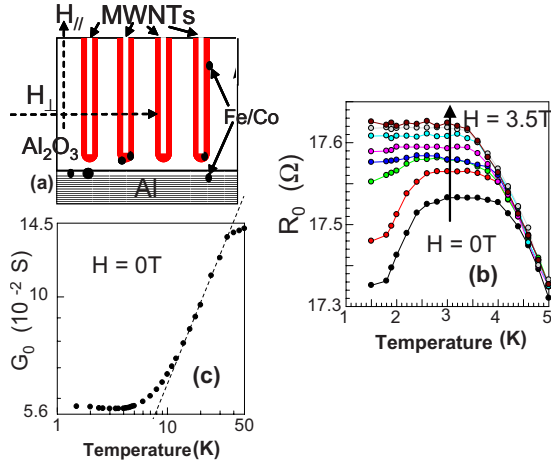


FIG. 1. (Color online) (a) Schematic cross-sectional view of the sample used for magnetization measurements. Au electrode and lead lines used for resistance measurements were detached. (b) Zero-bias resistance as functions of the temperature and magnetic field applied perpendicular to tube axis in partially end-bonded MWNTs (Ref. 6). (c) Doubly logarithmic scales of zero-bias conductance and temperature including the data in the temperature region shown in (b).

condition, we have investigated many synthesis conditions. As a result, we have found that deoxidization of Fe/Co catalyst by ($H_2 + Ar$) gas right before CVD process is the most effective to synthesize a large amount of MWNTs with high quality under the condition.

III. RESISTANCE MEASUREMENT: SIGN OF SUPERCONDUCTIVITY IN PARTIALLY END-BONDED MWNTs

Figure 1(b) shows zero-bias resistance (R_0) as functions of temperature (T) and magnetic fields (H) of the partially end-bonded MWNTs array.⁶ As temperature decreases, R_0 monotonically increases but it slightly and gradually drops below $T_{cR} = 3$ K at $H = 0$ T. As the field increases, this R_0 drop rapidly disappears.

As reported in our previous work,⁶ we found that the T_c values and behaviors of resistance drop were very sensitive to the number of layers (N) of a MWNT with current flow, which were controlled by contacts of top ends of MWNTs/Au electrodes. Only the entirely end-bonded MWNTs exhibited an abrupt resistance drop due to SC with the $T_c = 12$ K due to the largest N value ($N = 9$), while the partially end-bonded MWNTs resulted in only a slight and gradual resistance drop (i.e., sign of SC) at low T_c (e.g., $T_c < 4$ K) as shown in Fig. 1(b) owing to the smaller N values ($1 < N < 9$).

These N dependences were attributed to interaction between SC phase with a phonon-mediated attractive Coulomb interaction and Tomonaga-Luttinger liquid (TLL) state with a repulsive Coulomb interaction. The TLL state is a collective phenomenon (e.g., showing spin-charge separation) that arises from the repulsive Coulomb interaction between elec-

trons confined in a 1D ballistic conductance regime. Power laws in conductance vs energy relationships ($G \propto E^\alpha$) as shown in Fig. 1(c) can be evidence for TLL. The α value of ~ 0.5 is in good agreement with previous report of the TLL states in CNTs.⁶

Because TLL was strongly suppressed due to the inter-layer electrostatic coupling for a large value of $N = 9$ in the entirely end-bonded MWNTs, SC phase could abruptly appear at T_c as high as 12 K. In contrast, because strength of TLL and SC was comparable due to the smaller N value in the partially end-bonded MWNTs, only gradual resistance drop (sign of SC) at low T_c appeared as shown in Fig. 1(b). Because most samples exhibited this sign of SC, we have measured magnetization of these samples in the present report.

IV. MAGNETIZATION MEASUREMENTS

A. Measurement results

However, it should be noticed that the applied fields can drive the current in all the shells in any MWNTs (at least $\sim 10^4$) shown in Fig. 1(a) in the case of magnetization measurements. Because this results in the largest N values in the array, one can neglect influence of electrode contacts and TLL states. In this sense, T_{cH} , which arises from the largest N value in the array structure in the magnetization measurements, should become larger than T_{cR} . Indeed, after the resistance measurements, Au electrode and lead lines have been etched out as shown in Fig. 1(a) and magnetization of alumina template with MWNTs and Al substrate was measured, using superconducting quantum interference device (Quantum Design).

The inset of Fig. 2(a) shows the magnetization $M_\perp(T, H)$, as functions of the T and the H applied perpendicular to the longitudinal tube axis (H_\perp) in the sample for Fig. 1 in the zero-field cooled (ZFC) regime. As the field increases, the magnetization within positive values monotonically increases over the entire temperature range. This is attributed to very small volume of Fe/Co catalyst still remaining in some parts of the sample as shown in Fig. 1(a). Moreover, such small-volume Fe/Co catalyst also obstructed detection of the Meissner effect in the FC regime.

In contrast, the main panels of Figs. 2(a) and 2(b) show the normalized magnetization $M_{n\perp} = M_\perp(T, H) - M_\perp(T = 30 \text{ K}, H)$, obtained from the inset of Fig. 2(a). As the T decreases, very evident magnetization drop can be observed at $T < T_{cH} = 18 - 23$ K at $H = 30$ Oe. The amplitude of this drop increases monotonically with an increase in $H_\perp < 100$ Oe over all the T values $< 18 - 23$ K. Because no magnetization change is observable above $T = \sim 23$ K at $H = 30$ and 50 Oe, this magnetization drop is very distinct. In Fig. 2(b), the magnetization drop saturates at $H = \sim 100$ Oe, while $M_{n\perp}$ increases with an increase in $H_\perp > 100$ Oe over the entire T range.

Importantly, this gradual and unsaturated magnetization drop below $T_c = 18 - 23$ K occurs only in the samples that exhibit the sign of SC.⁶ This implies a possibility that the magnetization drop is strongly associated with Meissner dia-

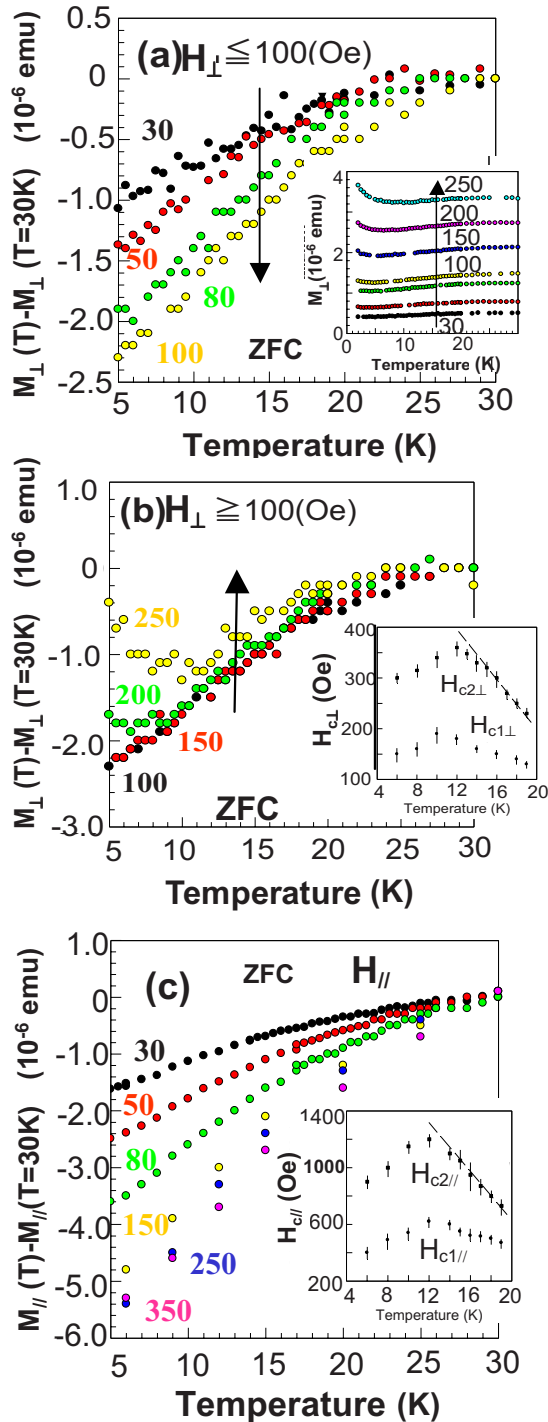


FIG. 2. (Color online) Normalized magnetization $M_{n\perp\parallel} = M_{\perp\parallel}(T, H) - M_{\perp\parallel}(T=30\text{K}, H)$, of the Fig. 1 sample. The number on each curve denotes the magnetic field (in Oe). (a) Results for $H_{\perp} < 100$ Oe and (b) $H_{\perp} > 100$ Oe. (c) Results for H_{\parallel} . Insets: (a) Non-normalized magnetization $M_{\perp}(T, H)$ of the sample used for main panel. (b), (c) Lower and upper critical fields (H_{c1} and H_{c2} , respectively) as a function of T for (b) perpendicular ($H_{c\perp}$) and (c) parallel ($H_{c\parallel}$) fields. The critical fields are determined from $M_{n\perp\parallel}$ vs H curves for different temperatures.

magnetization. As mentioned above, $M_{n\perp}(H)$ decreases below $H = \sim 100$ Oe and increases above it. These behaviors

are in qualitatively good agreement with Meissner effect for type-II superconductors.¹⁰

Figure 2(c) shows $M_{n\parallel}(H)$ for fields applied parallel to the longitudinal tube axis (H_{\parallel}) in the ZFC regime. Although magnetization drops are also evident, the value of T_{cH} interestingly becomes unclear in contrast to that in Fig. 2(a). Because of the H_{\parallel} , which corresponds to the application of fields within the graphene planes, the diamagnetism of graphite¹¹ that exists above T_{cH} in any samples (even from room temperature) becomes more significant than that in Fig. 2(a) (> 50 Oe) even at low fields in this case. The very gradual magnetization drop due to this graphite diamagnetism smears out presence of evident T_{cH} .

In Fig. 2(c), however, the drop saturates at $H_{\parallel} = \sim 250$ Oe [$\geq H_{\perp} = \sim 100$ Oe in Fig. 2(a)], while $M_{n\parallel}(H)$ starts to increase above $H_{\parallel} = \sim 250$ Oe. These behaviors also support Meissner effect for type-II superconductors as well as those in Figs. 2(a) and 2(b).

B. Critical fields and their temperature dependence

In order to confirm Meissner effect, we investigated the lower and upper critical fields (H_{c1} and H_{c2}). We have measured M vs T curves as a function of H with $\Delta H = 10$ Oe and produced M_n vs H curves at each temperature. From the H values showing the minimum M_n values and the $M_n = 0$ in the M_n vs H curves, H_{c1} and H_{c2} were estimated, respectively. The insets of Figs. 2(b) and 2(c) show the H_{c1} and H_{c2} as a function of T for fields applied (b) perpendicular ($H_{c\perp}$) and (c) parallel ($H_{c\parallel}$) to the tube axis. Importantly, H_{c1} and H_{c2} monotonically increase with a decrease in T value at $T > 12$ K, and $H_{c\perp}$ is also smaller than $H_{c\parallel}$. These results are in qualitatively good agreement with that reported for type-II superconductors within the Bardeen-Cooper-Schrieffer theory.¹⁰ It was also confirmed in C_6Ca ,^{1,2} C_6Yb ,¹ and boron-doped diamonds.³

From slope values of linear lines at $T > 12$ K in the insets of Figs. 2(b) and 2(c), the values of $H_{c2\perp}(T=0) = \sim 350$ Oe and $H_{c2\parallel}(T=0) = \sim 1100$ Oe can be estimated using the relationship $H_{c2\perp\parallel}(T=0) = -0.69(dH_{c2}/dT|_{T_c})T_c$, subtracting the values of H_{c1} and H_{c2} at $T_c = 19$ K that is not zero due to the diamagnetism of the graphite structure. The Ginzburg-Landau (GL) superconductive coherence length $\xi = [\Phi_0/2\pi H_{c2}(T=0)]^{1/2}$, where $\Phi_0 = h/2e$ is the quantum magnetic flux, can be estimated as $\xi_{\perp} = \sim 11$ nm and $\xi_{\parallel} = \sim 19$ nm from the $H_{c2\perp\parallel}(T=0)$. On the other hand, the penetration length of the magnetic field $\lambda = (m^*/\mu n_s e^2)^{1/2}$ is estimated as order of ~ 100 nm. This λ value is significantly larger than $\xi_{\perp} = \sim 11$ nm and $\xi_{\parallel} = \sim 19$ nm. This result apparently supports the fact that the present MWNTs are type-II superconductors. Furthermore, the values of ξ_{\perp} and ξ_{\parallel} are relevant in the order compared with those of $\xi_{\perp ab} = 13$ nm and $\xi_{\parallel ab} = 35$ nm in C_6Ca ,^{1,2} and $\xi = 10$ nm in boron-doped diamond,³ although they are slightly smaller.

Consequently, we conclude that the magnetization drops observed in Fig. 2 are attributed to Meissner effect for type-II superconductors. The gradual and unsaturated magnetization drops are typical behaviors in dirty superconductors with inhomogeneous carrier doping.^{1,3,12,13}

C. Unconventional behaviors

On the other hand, we notice some unconventional behaviors. (1) In the insets of Figs. 2(b) and 2(c), The values of H_c 's decrease at $T < \sim 12$ K as temperature decreases. This is due to the significant $M_{n\perp}$ increase in the $M_{n\perp}$ vs H curves with increasing H at each low temperature. This is attributed to Fe/Co catalyst still remaining in some part of the sample. (2) This remaining Fe/Co catalyst also obstructed appearance of magnetization drops in FC regime. (3) The values of H_c 's do not become zero even around $T_{cH} = 18\text{--}23$ K. This is due to the diamagnetism of the graphite structure of the MWNTs,¹¹ which is different from Meissner diamagnetism, existing at $T > \sim 23$ K. (4) Hence, the observed magnetization values here are sum of diamagnetism of graphite structures of MWNTs, Meissner diamagnetism, and ferromagnetism of Co/Fe catalyst. Thus, we cannot straightforwardly determine the volume fraction of Meissner diamagnetic contribution, although we estimated the volume fraction was about only 1% in the resistance measurements.⁶ (5) $T_{cH} = 18\text{--}23$ K in Fig. 2(a) was higher than $T_{cR} = 3$ K shown in Fig. 1. The highest $T_{cH} = 18\text{--}23$ K is even greater than the highest $T_{cR} = 12$ K reported in Ref. 6. These are because the applied fields can lead to the largest N in an array in magnetization measurements as mentioned in the introduction.

However, parasitic magnetisms such as (1)–(4) give mostly no influence to H_c at $T > 12$ K and our estimation of ξ . Therefore, in spite of such obstructions, we can still conclude Meissner effect in the present study.

D. Mechanisms and contribution of array structure

Here, we discuss the mechanisms of the observed Meissner effect. These small values of ξ clarify the dominant mechanism of the observed SC. At least, the following two origins for SC in CNTs have been theoretically reported to date. (1) Contribution of the large values of N in the case of ropes of SWNTs¹⁴ and the present MWNTs as discussed above.⁶ (2) Contribution of curvature (i.e., enhancement of electron-phonon interactions by formation of sp^3 hybrid orbitals) in very thin SWNTs.¹⁵ Indeed, some of the present MWNTs include such a very thin SWNT as the innermost shell.

However, the values of $\xi_{\perp} = \sim 11$ nm and $\xi_{\parallel} = \sim 19$ nm estimated above evidently indicate that the contribution of curvature in the thin innermost shell is not a dominant for the present case, because these values imply that the path of the shielding current for the Meissner effect and the vortex cannot be confined into the innermost shell with a diameter as small as ~ 0.5 nm. Moreover, we obtain $\Gamma(H_{c2}, T=0) = [(H_{c2\parallel} = 1100 \text{ Oe}) / (H_{c2\perp} = 350 \text{ Oe})] = \sim 3.1$ from the magnetic anisotropy measurements. This implies weak magnetic anisotropy with the 3D Fermi surface, as observed in C_6Yb [$\Gamma(H_{c2}, T=2 \text{ K}) = \sim 2$] and C_6Ca [$\Gamma(H_{c2}, T=0 \text{ K}) = \sim 1.6$].^{1,2} This also strongly supports the above-mentioned argument, because the diameter of 0.5 nm and length of ~ 600 nm of the innermost shell should result in considerably higher magnetic anisotropy. Therefore, we conclude that the contribution of the large N values should be the important factor for

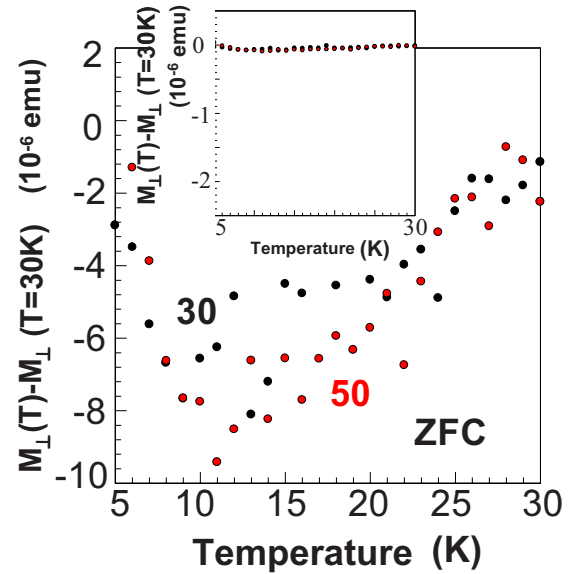


FIG. 3. (Color online) Normalized magnetization of MWNTs, which were placed on the Al substrate after dissolving alumina template, at $H = 30$ and 50 Oe in the ZFC. We dissolved the alumina template of the sample used for Fig. 2 by using an ethanol solution. Subsequently, the entire solutions were spin-coated at random on a pure Al substrate without any losses and, then, the magnetization was measured by applying a field perpendicular to the Al substrate and tube. Inset: Main panel figure shown with the same scales as those in the main panel of Fig. 2(a).

the present Meissner effect, although curvature of the innermost shell also contributes to production of Cooper pairs more or less.

Moreover, we notice that the large N values even in individual MWNTs may be not sufficient to explain Meissner effect, because the geometric anisotropy of the tube outer diameter and length is still large as compared with $\Gamma(H_{c2}, T=0) = \sim 3.1$ and the outer diameter of ~ 7 nm also is smaller than $\xi_{\perp} = \sim 11$ nm. From this standpoint, we investigated influence of intertube coupling in array structure. For this, the magnetization measurements were performed in MWNTs, which were placed on the Al substrate at random after dissolving the Al_2O_3 template. Figure 3 shows the result.

The magnetization shown in inset of Fig. 3 is two orders of magnitude less than that shown in Fig. 2(a) over the entire temperature range and the magnetization drop observed below $T = 18\text{--}23$ K in Fig. 2(a) disappears entirely. Although only very slight magnetization drop is observable from very high temperatures in the main panel, it is due to diamagnetism of graphite structure of MWNTs as mentioned for Fig. 1(b). This result implies that the intertube coupling in the honeycomb array of MWNTs is the dominant factor as well as the large N values for the present Meissner effect.¹⁶ Shielding current or vortex can exist crossing the MWNTs placed as the honeycomb array. This is just analogous to Abrikosov lattice for type-II superconductor.

The mean spacing between neighboring MWNTs is less than ~ 5 nm and some parts have MWNT spacing as small as ~ 3 nm as the minimum case. These thicknesses of Al_2O_3 ,

which is an insulator, are sufficient for the coupling of Cooper pair wave functions leaked by neighboring MWNTs or the tunneling of Cooper pairs. Indeed, we reported single electron tunneling through such thickness of Al_2O_3 barrier, which were attached at the ends of MWNTs in the same system in Ref. 17. In fact, it has been reported that the intertube coupling in ropes of SWNTs leads to (1) screening of the electron-electron interaction¹⁸ and (2) increase in the density of states by $\sim 7\%$ around E_F .¹⁹ These can be another reason for the present T_{cH} as high as ~ 20 K in addition to the contribution of the large N values.²⁰ In this sense, T_{cH} of individual MWNTs can be less than $T=5$ K.

V. POSSIBILITY OF INHOMOGENEOUS BORON DOPING

Finally, we notice that the gradual and unsaturated magnetization drop shown in Fig. 2 is typical behaviors in inhomogeneous superconductors such as C_6Ca ,¹ C_6S ,¹² boron-doped silicon,¹³ and boron-doped diamond.³ This indicates the possibility of inhomogeneous carrier doping into the present MWNT arrays. The weak magnetic anisotropy $\Gamma(H_{c2}, T=0) = \sim 3.1$, which suggested the 3D Fermi surface, also strongly supports this possibility. Moreover, all the shells in a MWNT should possess metallic behavior to obtain the $T_c (> \sim 10 \text{ K})$ ¹⁴ as well as a high density of states around Fermi level. This can be achieved by efficient carrier doping.

Although we have used boron only to activate the chemical reaction for deposition of Fe/Co catalyst, excess boron atoms will be inhomogeneously included into the carbon network during the growth of the array of MWNTs, occasionally. In fact, it was already reported that boron could be successfully doped into CNTs from catalyst including boron.^{21,22} The present case can be just analogous to these reports. Some reports also have theoretically predicted the doping effects in CNTs on superconductivity.^{23,24} In particular, Ref. 24 explained our SC and high T_c by carrier doping into MWNT with many Fermi points.

VI. CONCLUSION

We reported the gradual and unsaturated magnetization drops with an onset T_c of 18–23 K found in the honeycomb

arrays of MWNTs, which exhibited a slight resistance decrease due to the sign of superconductivity. The observed magnetic field dependence of the drops and temperature dependence of the critical fields indicated that it was attributed to Meissner effect for type-II superconductors. The T_c value of 18–23 K was the highest among those in the new carbon-related superconductors. The weak magnetic anisotropy, superconductive coherence length (11–19 nm), and disappearance of the Meissner effect after destructing array structure suggested a possibility that the intertube coupling of MWNTs in the honeycomb array was the dominant factor for the mechanism. Drastic reduction of ferromagnetic catalyst for the synthesis of the MWNTs allowed these finding.

Further investigation is, however, indispensable to fully reveal some unconventional behaviors (avoiding influence of parasitic magnetisms; e.g., Fe/Co catalyst) and also consistently understand all the properties of the SC observed in the present and previous studies.⁶ The large N values, curvature of the thin innermost shell in individual MWNTs, and the intertube coupling in the honeycomb array are expected to yield higher T_c values similar to those in C_{60} clusters and MgB_2 , by combining with controlled efficient boron doping.

Finally, it should be noticed that Bandow and Iijima *et al.* reported gradual and unsaturated magnetization drops with $T_c = \sim 20$ K, which has behaviors very similar to the present case, in the sheet of boron-doped high-quality MWNTs that were synthesized without using catalyst.²⁵ This strongly suggests high potentiality of assemblies (i.e., sheets, arrays, and ropes) of boron-doped MWNTs for yielding high- T_c SC.

ACKNOWLEDGMENTS

We are grateful to J. Gonzales, H. Bouchiat, C. Schonenberger, R. Egger, M. Dresselhaus, D. Tomanek, C. Shtrunk, J.-P. Leburon, H. Fukuyama, J. Akimitsu, T. Ando, S. Saito, R. Saito, and S. Bandow for their fruitful discussions and for providing encouragement during the present study. We also thank Y. Muranaka, Y. Oguro, and Y. Iye (ISSP, Tokyo University) for their valuable technical assistance in performing the SQUID measurements.

*J-haru@ee.aoyama.ac.jp

¹T. E. Weller *et al.*, Nat. Phys. **1**, 39 (2005).

²N. Emery, E. Demler, and E. Kaxiras, Phys. Rev. Lett. **95**, 087003 (2005).

³E. A. Ekimov, M. Y. Sfeir, L. Huang, X. M. Henry Huang, Y. Wu, J. Kim, J. Hone, S. O'Brien, L. E. Brus, and T. F. Heinz, Nature (London) **428**, 542 (2004).

⁴M. Kociak, S. Saito, and D. Tomanek, Phys. Rev. Lett. **86**, 2416 (2001).

⁵M. Ferrier, F. Ladieu, M. Ocio, B. Sacépé, T. Vaugien, V. Pichot, P. Launois, and H. Bouchiat, Phys. Rev. B **73**, 094520 (2006).

⁶I. Takesue, J. Haruyama, N. Kobayashi, S. Chiashi, S. Maruyama, T. Sugai, and H. Shinohara, Phys. Rev. Lett. **96**, 057001 (2006).

⁷Z. K. Tang *et al.*, Science **292**, 2462 (2001).

⁸Recently, only the first group has reported possible Meissner effect (Ref. 5).

⁹N. Murata *et al.* (unpublished).

¹⁰M. Tinkam, *Introduction to Superconductivity* (McGraw-Hill, New York, 1996).

¹¹S. Bandow, J. Appl. Phys. **80**, 1020 (1996).

¹²R. R. da Silva, J. H. S. Torres, and Y. Kopelevich, Phys. Rev. Lett. **87**, 147001 (2001).

¹³E. Bustarret *et al.*, Nature (London) **444**, 465 (2006).

¹⁴J. Gonzalez, Phys. Rev. Lett. **88**, 076403 (2002); **87**, 136401 (2001).

¹⁵R. Barnett, E. Demler, and E. Kaxiras, Phys. Rev. B **71**, 035429 (2005).

- ¹⁶Although we have measured magnetization of many undissolved and dissolved empty alumina templates, no magnetization drop has been observed in any samples.
- ¹⁷J. Haruyama, I. Takesue, T. Hasegawa, and Y. Sato, *Phys. Rev. B* **63**, 073406 (2001); *Appl. Phys. Lett.* **77**, 2891 (2000).
- ¹⁸F. Wang, M. Y. Sfeir, L. Huang, X. M. H. Huang, Y. Wu, J. Kim, J. Hone, S. O'Brien, L. E. Brus, and T. F. Heinz, *Phys. Rev. Lett.* **96**, 167401 (2006).
- ¹⁹Y.-K. Kwon, S. Saito, and D. Tománek, *Phys. Rev. B* **58**, R13314 (1998).
- ²⁰We reported the critical current behaviors following the GL theory (Ref. 6). Because this theory is applicable only to the 3D regime, this result is consistent with the theory. This indicates that transitions from the TLL to the superconducting phases at T_{cR} (Ref. 6) may be the 1D–quasi-1D (or 3D) phase transitions.
- ²¹K. McGuire *et al.*, *Carbon* **43**, 219 (2005).
- ²²K. Liu, Ph. Avouris, R. Martel, and W. K. Hsu, *Phys. Rev. B* **63**, 161404(R) (2001).
- ²³A. Sédéki, L. G. Caron, and C. Bourbonnais, *Phys. Rev. B* **65**, 140515(R) (2002).
- ²⁴E. Perfetto and J. Gonzalez, *Phys. Rev. B* **74**, 201403(R) (2006).
- ²⁵S. Bandow, S. Numao, and S. Iijima, *J. Phys. Chem. C* **111**, 11763 (2007).